Characterization of Anthozoan-Specific Opsins from a Reef-Building Coral, Acropora tenuis, as Gq-Coupled Opsins

Authors: Iwasaki, Makoto, Sakai, Yusuke, Shirata, Taishi, Sugihara, Tomohiro, Koyanagi, Mitsumasa, et al.

Characterization of Anthozoan-Specific Opsins From a Reef-Building Coral, *Acropora tenuis*, as Gq-Coupled Opsins

Makoto Iwasaki[1][†], Yusuke Sakai[1][†], Taishi Shirata[2], Tomohiro Sugihara[1], Mitsumasa Koyanagi[1,3], and Akihisa Terakita[1,3]*

[1]*Department of Biology, Graduate School of Science, Osaka Metropolitan University 3-3-138 Sugimoto, Sumiyoshi-Ku Osaka 558-8585, Japan*
[2]*Department of Biology and Geosciences, Graduate School of Science, Osaka City University, 3-3-138 Sugimoto, Sumiyoshi-Ku, Osaka 558-8585, Japan*
[3]*The OMU Advanced Research Institute for Natural Science and Technology, Osaka Metropolitan University, Osaka, Japan*

Most animals capture light through opsins, which are light-sensitive G protein-coupled receptors (GPCRs). Recent genome analyses of anthozoans, including corals and sea anemones, have identified novel opsins that are phylogenetically classified into two groups distinct from previously known opsin groups. Despite their significance in clarifying biological functions, the specific molecular properties of these opsins remain largely unknown. In this study, we investigated the G protein activations and biochemical responses light-dependently induced by two anthozoan opsins, Antho2a and Antho2d, obtained from the reef-building coral *Acropora tenuis*, in mammalian cultured cells. Using jumping spider Rh1 (SpiRh1), which belongs to a known Gq-type G protein (Gq)-coupled opsin group as a control, we observed that Antho2a and Antho2d elicited light-dependent increases in Ca^{2+} levels in cultured cells. This response was inhibited by a Gq inhibitor, indicating that these opsins activated Gq in a light-dependent manner. Interestingly, Antho2d also activated the Gi-type G protein (Gi), similar to SpiRh1, while Antho2a showed limited or negligible Gi activation. We also found that Gi activation additionally contributed to the Ca^{2+} elevation, suggesting it enhances Gq-dependent Ca^{2+} elevation in Antho2d- and SpiRh1-expressing cells. In contrast, Antho2a demonstrated a higher specificity for Gq activation compared to SpiRh1 and was nearly equivalent to hM3Dq, a GPCR known for its strong Gq specificity and widely used as a chemogenetic tool for manipulating Gq activation. Our results suggest that this new anthozoan opsin group consists of Gq-coupled opsins with varying levels of Gi activation, demonstrating their potential for optogenetic applications.

Key words: Anthozoa, coral, opsin, G protein, calcium

INTRODUCTION

Animal opsins bind to retinal chromophores to form light-sensitive pigments, most of which drive intracellular signaling by activating heterotrimeric G proteins in a light-dependent manner, leading to cellular responses. Animal opsins are categorized as members of G protein-coupled receptors (GPCRs). Thousands of opsins have been identified from a wide variety of animals, including chordates, arthropods, and cnidarians thus far and they are divided into eight groups (Terakita, 2005; Koyanagi and Terakita, 2014; Terakita and Nagata, 2014). Accumulated evidence suggests that members belonging to different groups activate different types of G proteins; for example, members of the protostome visual opsin/deuterostome melanopsin group, Gs-coupled cnidarian opsin group, and chordate visual/non-visual opsin group, couple to Gq-, Gs-, and Gi-type (transducin) G proteins, respectively (The heterotrimeric G protein composed of Gαx and βγ subunits is referred to as Gx.)

Recently, novel opsins have been discovered in anthozoan animals (under the phylum *Cnidaria*) such as corals and sea anemones. These opsins have been classified into two groups: anthozoan-specific opsin (ASO)-I and ASO-II, which are phylogenetically distinct from the eight known groups (Hering and Mayer, 2014; Gornik et al., 2021). In sea anemones and corals, both ASO-I and -II group members have been reported to be expressed in multiple tissues (Gornik et al., 2021; McCulloch et al., 2023; Shi et al., 2024). However, their physiological functions remain unknown, despite documented light-dependent behaviors and physiologies in these organisms (Dubinsky and Falkowski, 2011; Sakai et al., 2020; Lilly et al., 2024). More recently, we suc-

cessfully expressed a member of the ASO-II group, acropsin 4, from the reef-building coral *Acropora millepora* in mammalian cultured cells. We observed a light-dependent increase in Ca^{2+} levels in acropsin 4–expressing cultured cells, suggesting that ASO-II group members may activate Gq (Mason et al., 2023).

It is widely accepted that the protostome visual opsin/ deuterostome melanopsin group is a large group of Gq-coupled opsins (Koyanagi and Terakita, 2008), referred to as the bilaterian conventional Gq-coupled opsin group. Opsins in this group colocalize and/or functionally couple with Gq in the visual cells of various protostomes, including arthropods (Terakita et al., 1993; Lee et al., 1994; Nagata et al., 2012), as well as in intrinsically photosensitive retinal ganglion cells in mammals (Graham et al., 2008) and certain types of photoreceptor cells in amphioxus (Koyanagi et al., 2005). Opsins from this group elevate intracellular Ca^{2+} via activating Gq and phospholipase Cs in mammalian cultured cells (Sun et al., 2014) and they activate Gq in vitro in a light-dependent manner (Terakita et al., 1993, 2008). Interestingly, jumping spider Rh1 (SpiRh1) (Koyanagi et al., 2008; Nagata et al., 2012), which we propose using as a model for Gq-coupled opsins due to the availability of its crystal structure (Varma et al., 2019), mutant analysis (Nagata et al., 2019), and potential for optogenetic application (Hagio et al., 2023), has been reported to activate Gi as well as Gq in mammalian cultured cells (Varma et al., 2019). Mammalian melanopsin has also been shown to activate not only Gq but also Gi and Gs in mammalian cultured cells (Bailes and Lucas, 2013; McDowell et al., 2022). Therefore, it is of interest to investigate the activation of various G protein types, including Gq, by members of the ASO-II group. This will help to reveal their activation specificities and allow for comparison with those of members of the protostome visual opsin/ deuterostome melanopsin group.

Here, we investigated the light-dependent changes in second messengers and the G protein activation by two members (Antho2a and Antho2d) belonging to the ASO-II group from the reef-building coral *Acropora tenuis* as well as SpiRh1 from the protostome visual opsin/ deuterostome melanopsin group (Koyanagi et al., 2008), used as a control. We selected Antho2a and Antho2d as representatives for each of the two phylogenetically classified subgroups within the ASO-II group, subtype 1 and subtype 2.1, respectively (Gornik et al., 2021; Sakai et al., 2025, in press). We heterologously expressed these opsins in mammalian cultured cells and demonstrated that Antho2a and Antho2d light-dependently elevated Ca^{2+} levels in the cells via activation of Gq, suggesting that members of the ASO-II group are Gq-coupled opsins. Interestingly, Antho2d also activated Gi, similar to SpiRh1, while Antho2a showed lim-

ited or negligible Gi activation. We also found that Gi activation increased the magnitude of Ca^{2+} elevation triggered by Gq activation in Antho2d- or SpiRh1-expressing cells, suggesting that Gi activation enhances Gq-dependent Ca^{2+} elevation. Additionally, we investigated the activation specificity of Antho2a for various types of G proteins and compared it to hM3Dq, a Designer Receptors Exclusively Activated by Designer Drugs modified from the human M3 muscarinic receptor, Gq DREADD. hM3Dq is known for its high specificity for Gq over other types of G protein and is widely used as a chemogenetic tool for manipulating Gq (Armbruster et al., 2007).

MATERIALS AND METHODS

Construction of expression vectors of opsins

cDNAs of two *A. tenuis* opsins in the ASO-II group, Antho2a and Antho2d (Accession numbers LC844932 and LC844935, respectively), were isolated in a separate study (Sakai et al., 2025, in press). These opsins, along with jumping spider Rh1 (SpiRh1) (Koyanagi et al., 2008), were tagged with the epitope sequence of the anti-bovine rhodopsin monoclonal antibody rho 1D4 (ETSQVAPA) (Molday and MacKenzie, 1983) at their C-termini as described previously (Nagata et al., 2012). The tagged cDNAs of the *A. tenuis* opsins were inserted into the pMT expression vector (Shibahara et al., 1986), which was digested with *Eco* RI and *Not* I. The tagged cDNA of SpiRh1 was inserted into the pUSRα expression vector (Kayada et al., 1995), which was digested with *Hind* III and *Eco* RI.

Measurements of intracellular Ca^{2+} and cAMP levels

Changes in intracellular Ca^{2+} and cAMP levels in opsin-expressing HEK293S cells were measured using the aequorin assay and the GloSensor cAMP assay (Promega), respectively, as described previously (Koyanagi et al., 2013, 2022; Sugihara et al., 2016) with minor modifications. Briefly, 1.5 μg of each opsin plasmid
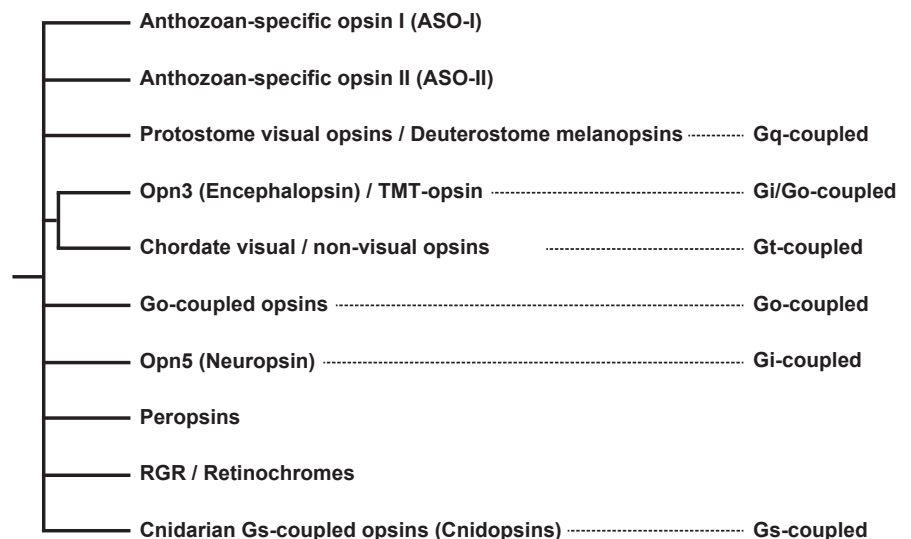

Fig. 1. Schematic illustration of animal opsin groups. This schematic illustrates the eight established opsin groups (Koyanagi and Terakita, 2014) and two anthozoan-specific opsin groups recognized in several published studies (Hering and Mayer, 2014; Gornik et al., 2021; Mason et al., 2023). The types of G proteins to which each opsin group is primarily coupled are also shown. Note that it was reported some members of Opn5 group activated Gq group G proteins (Wagdi et al., 2022; Sato et al., 2023). Antho2a and Antho2d are categorized under the ASO-II group, while jumping spider Rh1 (SpiRh1) is a member of the protostome visual opsin group.

was transfected into HEK293S cells with 1.5 µg of either the aequorin plasmid or the pGloSensor-20F cAMP plasmid (Promega), using the polyethyleneimine (PEI) transfection method. The aequorin used in this study was obtained by introducing a reverse mutation, A119D, into the plasmid [pcDNA3.1+/mit-2mutAEQ] (Addgene #45539) (De La Fuente et al., 2012; Koyanagi et al., 2022). After transfection, the cells were incubated for 4 h (for the aequorin assay) or overnight (for the GloSensor cAMP assay), then treated with 11-*cis* retinal and further incubated overnight at 37°C. Before measurements, the culture medium was replaced with a CO_2-independent medium containing 10% FBS and Coelenterazine *h* (Wako) for the aequorin assay or GloSensor cAMP Reagent stock solution (Promega) for the GloSensor assay. The cells were incubated for at least 2 h to equilibrate with the media. Luminescence values were measured at 25°C using GloMAX 20/20n Luminometers (Promega). The cells were illuminated with green light (Dual Head LED Light 495 nm or 506 nm, GB Life Science) for 1 s in both assays. It should be noted that Antho2a and Antho2d were suggested to form green light-sensitive pigments (Sakai et al., 2025, in press for Antho2a; see Supplementary Figure S1 for Antho2d), like SpiRh1 (Nagata et al., 2012). For Gq inhibition, YM-254890 (Wako) diluted in dimethyl sulfoxide (DMSO; final concentration of 1 µM) was added more than 5 min before the measurement. For Gi/Go inhibition, pertussis toxin (PTX) (Wako) diluted in a buffer containing 10 mM potassium phosphate, 137 mM NaCl, and 10% glycerol (final concentration of 200 µg/mL) was added just before the supplementation of 11-*cis* retinal and when replacing the culture medium with the CO_2-independent medium.

Measurement of G protein activation

    Light-dependent G protein activations by opsins in HEK293S cells were investigated using the NanoBiT-G-protein dissociation assay (Inoue et al., 2019). 2.4 µg of each opsin plasmid was transfected into HEK293S cells with 0.06 µg of Gα-LgBiT, 0.3 µg of Gβ1-SmBiT, and 0.3 µg of Gγ2 plasmids using the PEI transfection method, as described in a previous report (Matsuo et al., 2023). In the experiments comparing G protein activations by Antho2a or SpiRh1 with those by hM3Dq, 1.2 µg of each opsin plasmid and 1.2 µg of hM3Dq (Gq DREADD) (Armbruster et al., 2007) plasmid were transfected into HEK293S cells with 0.06 µg of Gα-LgBiT, 0.3 µg of Gβ1-SmBiT, and 0.3 µg of Gγ2 plasmids. The transfected cells were incubated overnight at 37°C. Before measurements, the culture medium was replaced with a CO_2-independent medium containing 10% FBS, Nano-Glo Vivazine Substrate (Promega), and 11-*cis* retinal, and the cells were incubated for at least 4 h to equilibrate with the media. Luminescence values were measured at 25°C using a GloMAX 20/20n Luminometer (Promega). The cells were illuminated with green LED light (495 nm) for 5 s. An agonist of hM3Dq, clozapine *N*-oxide (CNO; R&D Systems, Inc.; final concen-

tration of 0.2 µM), was added to stimulate hM3Dq. The G-alpha subunit sequences used for the Gα-LgBiT constructs are as follows: human Gαq (GenBank accession number: NP_002063.2), human Gα11 (NP_002058.2), human Gα14 (NP_004288.1), human Gαz (NP_002064.1), human Gα12 (NP_031379.2), human Gα13 (NP_006563.2), human Gαs (NP_000507.1), human Gαolf (NP_892023.1), rat Gαi1 (NP_037277.1), rat Gαi2 (NP_112297.1), rat Gαi3 (NP_037238.1), mouse Gα15 (NP_034434.1), mouse GαoB (NP_001106855.1), mouse Gαt1 (NP_032166.1), mouse Gαt2 (NP_032167.1), mouse Gαt3 (NP_001074612.1), monkey GαoA (NP_001182358.1) and zebrafish Gαv (NP_001159486.1). The G-beta subunit sequence used for the Gβ1-SmBiT construct was derived from human Gβ1 (NP_001269468.1), and the Gγ2 sequence was derived from human Gγ2 (NP_001230702.1). The GαoA-LgBiT, Gβ1-SmBiT, and Gγ2 plasmids were provided by Dr. Takashi Nagata and Dr. Keiichi Inoue (The University of Tokyo) (Matsuo et al., 2023). The other Gα-LgBiTs were constructed based on the nucleotide sequence of GαoA-LgBiT.
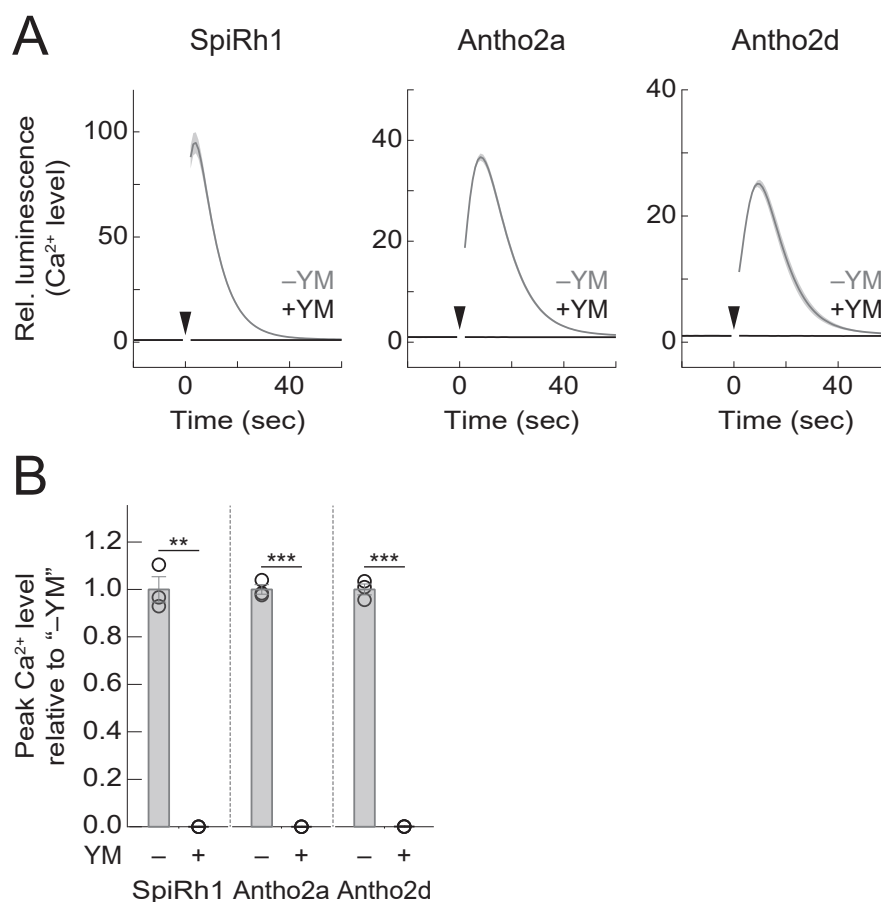

Fig. 2. Light-dependent changes in Ca^{2+} levels in Antho2a-, Antho2d-, and SpiRh1-expressing HEK293S cells. **(A)** Time courses of changes in intracellular Ca^{2+} levels were measured with (black curves) and without (gray curves) the Gq inhibitor YM-254890 (denoted as YM in each graph) using the aequorin-based Ca^{2+} sensor. Data are presented as mean (solid curves) ± SEM (shading) for $n = 3$ replicates. Black arrowheads indicate the timing of irradiation with green light (495 nm, for 1 s, 4.30×10^{16} photons/cm²/s). Luminescence values were normalized to the average of the 6 s immediately prior to irradiation (= relative luminescence). **(B)** Effect of YM-254890 on the peak Ca^{2+} response in opsins-expressing HEK293S cells. The peak relative luminescence values were normalized to the average of those without YM ("−YM") for each opsin. Each bar graph, with error bars, shows the mean ± SEM for $n = 3$ replicates. Open circles indicate individual records. Welch's *t*-test was used to compare results with and without YM for each opsin (**$P < 0.01$, ***$P < 0.001$).

RESULTS

Light-dependent Ca^{2+} and cAMP changes induced by Antho2a and Antho2d

We expressed two opsins from *A. tenuis*, Antho2a and Antho2d, both belonging to the ASO-II group (Fig. 1), in HEK293S cells and analyzed light-dependent changes in Ca^{2+} levels in these cells using the Ca^{2+}-sensitive luminescent protein aequorin. We also included jumping spider Rh1 (SpiRh1), a member of the protostome visual opsin/deuterostome melanopsin group and one of the well-studied opsins (Koyanagi and Terakita, 2008; Koyanagi et al., 2008; Nagata et al., 2012, 2019; Varma et al., 2019), as a control in the luminescence assay. Both Antho2a- and Antho2d-expressing cells exhibited a clear increase in luminescence intensity upon light irradiation, indicating a light-dependent increase in Ca^{2+} levels (Fig. 2A, gray curves). This light-dependent Ca^{2+} elevation was consistent with our previous observation that acropsin 4, an ASO-II group opsin from another coral species (*A. millepora*), light-dependently elevated Ca^{2+} levels in mammalian cultured cells (Mason et al., 2023). We used YM-254890 (Taniguchi et al., 2003), a specific inhibitor for activation of Gq-group G proteins (Gq, G11, G14) (Zhang et al., 2020), to investigate whether the increase in intracellular Ca^{2+} levels was due to Gq activation by each opsin. The light-dependent Ca^{2+} increase was completely abolished under the presence of YM-254890 in Antho2a-, Antho2d-, and SpiRh1-expressing cells (Fig. 2A, black curves and Fig. 2B), suggesting that Antho2a and Antho2d activate G proteins of the Gq-group, similar to SpiRh1. In other words, the activation of the member(s) of Gq group is essential for the light-dependent Ca^{2+} elevation by Antho2a and Antho2d, just as it is for SpiRh1.

SpiRh1 has been reported to activate Gi in addition to Gq (Varma et al., 2019). Therefore, we analyzed the decrease in intracellular cAMP levels in Antho2a- and Antho2d-expressing cells using cAMP-sensitive luciferase (GloSensor^{TM}, Promega) to investigate light-dependent activation of Gi, as it is well known that Gi suppresses adenylyl cyclase activity. We observed a clear transient decrease in cAMP levels in SpiRh1-expressing cells upon light irradiation, while Antho2a- and Antho2d-expressing cells did not show a clear decrease in cAMP levels (Fig. 3, gray curves). The addition of PTX, an inhibitor of activation of members of the Gi group (Gi and Go) by GPCRs, altered the cAMP change profiles significantly in both Antho2d- and SpiRh1-expressing cells, although the profiles after PTX treatment are different from each other (Fig. 3, black curves). In contrast, no clear change in the profile was observed in Antho2a-expressing

cells after PTX treatment (Fig. 3, black curves). The "difference profiles" comparing between the presence and absence of PTX clearly indicated a Gi/Go-dependent decrease in cAMP levels in both SpiRh1- and Antho2d-expressing cells, although their detailed profiles were different (Fig. 3, broken black curves). However, there was no detectable decrease in Antho2a-expressing cells (Fig. 3, broken black curves). These results suggest that Antho2d, like SpiRh1, activates Gi/Go, while Antho2a shows limited or negligible activation of Gi/Go. It should be noted that in the presence of PTX, the light-dependent increase of cAMP was observed in SpiRh1- and Antho2d-expressing cells (Fig. 3, black curves), which is discussed in the DISCUSSION section.

Next, we evaluated the contribution of Gi/Go activation to the light-dependent Ca^{2+} elevation in Antho2d-expressing cells, comparing it to Antho2a, which has almost no Gi/Go activation ability, and SpiRh1, which clearly activates Gi/Go. We investigated the effects of Gi/Go inhibition by PTX on the Ca^{2+} response in each of the opsin-expressing cells. The addition of PTX resulted in a partial reduction of the Ca^{2+} increase in both Antho2d- and SpiRh1-expressing cells, whereas no effect of the Gi/Go inhibitor was observed in Antho2a-expressing cells (Fig. 4A, B). This indicates that Gi/Go activation is involved in the pathway leading to the light-dependent Ca^{2+} increase in Antho2d- and SpiRh1-expressing cells. Together with the finding that the Gq inhibitor completely abolished the light-dependent Ca^{2+} increase in Antho2d- and in SpiRh1-expressing cells (Fig. 2), this suggests that while Gi/Go activation is not essential for the light-dependent Ca^{2+} increase by Antho2d, or SpiRh1, it does make a significant additional contribution to the Ca^{2+} increase triggered by Gq activation (see the DISCUSSION section).
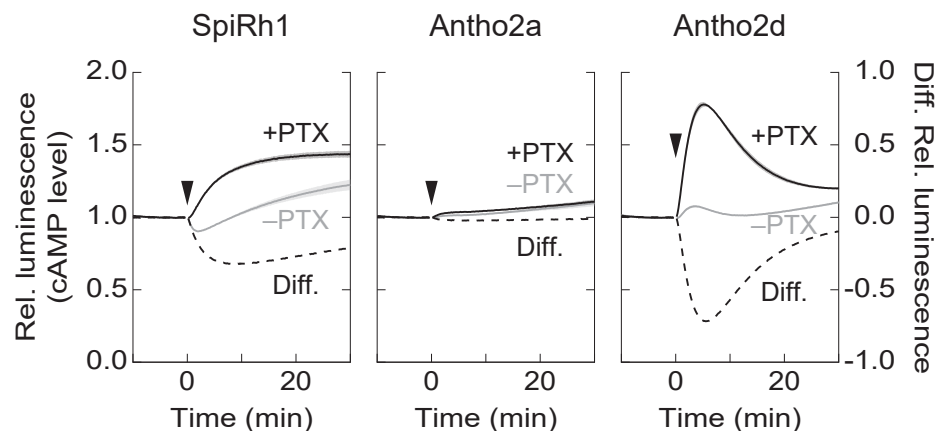

Fig. 3. The effect of Gi/Go inhibition on light-dependent changes in cAMP levels in Antho2a-, Antho2d-, and SpiRh1-expressing HEK293S cells. Time courses of the changes in intracellular cAMP levels were measured in the presence (black curves) and absence (gray curves) of the Gi/Go inhibitor pertussis toxin (denoted as PTX in each graph), using the GloSensor 20F cAMP sensor. Data are presented as mean (solid curves) ± SEM (shading) for *n* = 3 replicates. Luminescence values were normalized to the average of the 60 s immediately prior to irradiation (= relative luminescence). The difference profiles ("Diff.") between the conditions with and without PTX (calculated by subtracting the relative luminescence values of "+PTX" from those of "–PTX") are shown as broken black curves. Black arrowheads indicate the timing of irradiation with green light (506 nm, for 1 s, 6.13 × 10^{16} photons/cm^2/s). To eliminate any effects of Gq activation on intracellular cAMP changes, these experiments were conducted in the presence of YM-254890.
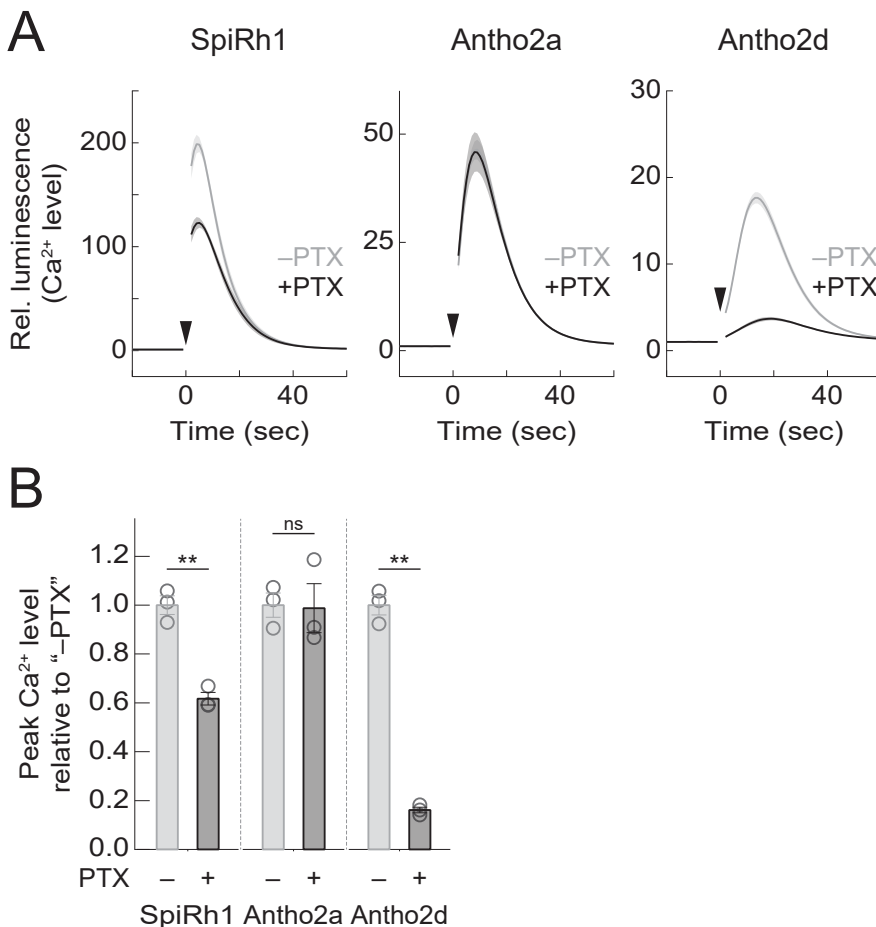
A

SpiRh1 | Antho2a | Antho2d

B

Fig. 4. The effect of Gi/Go inhibition on light-dependent changes in Ca^{2+} levels in Antho2a-, Antho2d-, and SpiRh1-expressing HEK293S cells. **(A)** Time courses of changes in intracellular Ca^{2+} levels were measured with (black curves) and without (gray curves) PTX using the aequorin-based Ca^{2+} sensor. Data are presented as mean (solid curves) $\pm$ SEM (shading) for $n = 3$ replicates. Black arrowheads indicate the timing of irradiation with green light (495 nm, for 1 s, 4.30×10^{16} photons/cm^2/s). Luminescence values were normalized to the average of the 6 s immediately prior to irradiation (= relative luminescence). **(B)** Effect of PTX on the peak Ca^{2+} response in opsin-expressing HEK293S cells. The peak relative luminescence values were normalized to the average of those without PTX ("–PTX") for each opsin. Each bar graph, with error bars, shows the mean $\pm$ SEM for $n = 3$ replicates. Open circles indicate individual records. Welch's t-test was used to compare results with and without PTX for each opsin ("ns" not significant, **$P < 0.01$).

Observation of G protein activation by Antho2a

The results presented in Figs. 3 and 4 suggest that Antho2a activates Gi/Go only minimally or negligibly. We therefore investigated the activation of members of the Gi group by Antho2a using the NanoBiT-G-protein dissociation assay (Inoue et al., 2019). Antho2a clearly activated members of the Gq group, which are known as PLCβ activators (Hubbard and Hepler, 2006), similar to SpiRh1; specifically, it activated G14 more strongly and Gq and G11 to a lesser extent compared with SpiRh1 (Fig. 5A, and see Supplementary Figure S2A). In contrast, while SpiRh1 activated all tested members of the Gi group (Gi1, Gi2, Gi3, Gz, GoA, GoB, Gt1, Gt2, and Gt3), Antho2a showed only slight activation of GoA, GoB, and Gz, with no clear activation observed for the other members of the Gi group (Fig. 5B, and see Supplementary Figure S2B). This limited activation ability of

Antho2a for members of the Gi group is consistent with the absence of PTX effects on light-dependent cAMP and Ca^{2+} changes in Antho2a-expressing cells (Figs. 3, 4). We also confirmed that the presence of PTX did not change the efficiency of Gq activation by either Antho2a or SpiRh1 (see Supplementary Figure S3), indicating that the PTX effect on light-dependent Ca^{2+} elevation in SpiRh1 was associated with Gi/Go activation by SpiRh1.

We also analyzed the activation of the members of G protein groups other than Gq and Gi, specifically, members of the Gs, G12, and Gv groups, by Antho2a compared to SpiRh1 (see Supplementary Figure S2C–E). (Gv is the fifth Gα protein group and is conserved across the animal kingdom, including arthropods, mollusks, and annelids (Oka et al., 2009).) Neither Antho2a nor SpiRh1 significantly activated members of these three groups, with one exception: both opsins efficiently activated G12 (see Supplementary Figure S2D). This finding is consistent with previous observations that several Gq-coupled GPCRs can efficiently activate G12 (Gohla et al., 2000; McCoy et al., 2010).

Comparison between the activation specificities of Antho2a and hM3Dq for various G proteins

The results presented above showed that among various types of G proteins, Antho2a exhibits a higher specific activation ability for the Gq group G proteins. hM3Dq is known as a GPCR with high Gq-specific activation ability and serves as a chemogenetic tool to selectively manipulate Gq activation in target cells (Armbruster et al., 2007). The effects of YM-254890 and PTX on agonist-dependent Ca^{2+} increases in hM3Dq-expressing cells (see Supplementary Figure S4A, B) were very similar to those observed for light-dependent Ca^{2+} increases in Antho2a-expressing cells (Figs. 2A, 4A). Therefore, we attempted to compare the activation abilities of Antho2a and hM3Dq for various G proteins, including members of G protein groups other than Gq and Gi, specifically the Gs, G12, and Gv groups.

We co-expressed Antho2a and hM3Dq in cultured cells and comparatively analyzed G protein activation upon light and hM3Dq-agonist stimulations, respectively. The amount of each type of G protein activated by hM3Dq and Antho2a was plotted on a two-dimensional graph, with hM3Dq and Antho2a values on the horizontal (x-axis) and vertical (y-axis) axes, respectively (Fig. 6). In the graph, the line connecting the origin and the point of Gq activation is represented by a
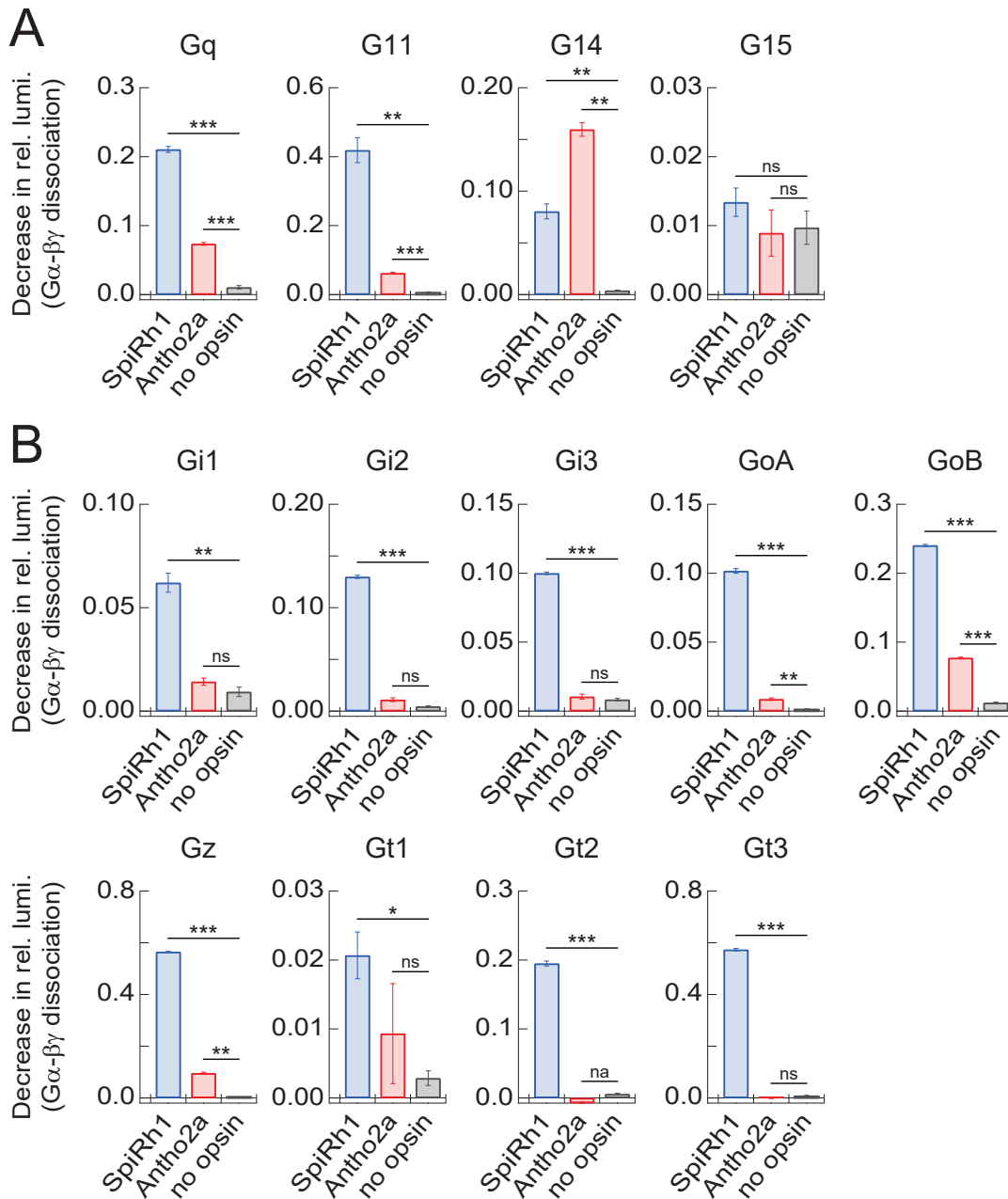
Fig. 5. Activations of the Gq- and Gi-group G proteins by SpiRh1 and Antho2a. Light-dependent activations of members of the Gq group **(A)** and Gi group **(B)** G proteins by SpiRh1 and Antho2a were measured using the NanoBiT-G-protein dissociation assay. G protein activation (Gα-βγ dissociation) was measured as a decrease in relative luminescence upon light irradiation in HEK293S cells co-expressing each Gα with Antho2a or SpiRh1 (see Materials and Methods and Supplementary Figure S2 for details). Each graph indicates the maximum decrease in relative luminescence over a 10-minute period after light irradiation. The time courses of the relative luminescence changes used to create this figure are shown in Supplementary Figure S2A and B. Each bar graph, with error bars, shows the mean ± SEM for $n = 3$ replicates. Welch's t-test was used to compare results between opsin-expressing cells and no-opsin-expressing cells ("ns" not significant, *$P < 0.05$, **$P < 0.01$, ***$P < 0.001$, "na" not activated: significant, but lower than that of no opsin).

tentative linear equation, $y = f(x)$ (broken line). If the activation value of a certain G protein is plotted on the line, it indicates that the activation ability for that G protein relative to Gq is identical between Antho2a and hM3Dq. If Antho2a exhibits higher or lower activation abilities for given G proteins compared to hM3Dq, the points are plotted in regions where $y > f(x)$ (orange background) or $y < f(x)$ (green background), respectively. For members of the Gq group, both

Antho2a and hM3Dq clearly activated Gq, G11, and G14, and Antho2a showed higher or lower activation abilities for G14 or G11 relative to Gq compared to hM3Dq, respectively (red open circles in Fig. 6). Although the activation profiles of Gq group G proteins differed between Antho2a and hM3Dq, it was evident that Antho2a efficiently activated Gq group G proteins. The six subtypes of the Gi group and G12 were plotted in the area of $y < f(x)$ or roughly on the line of $y = f(x)$,
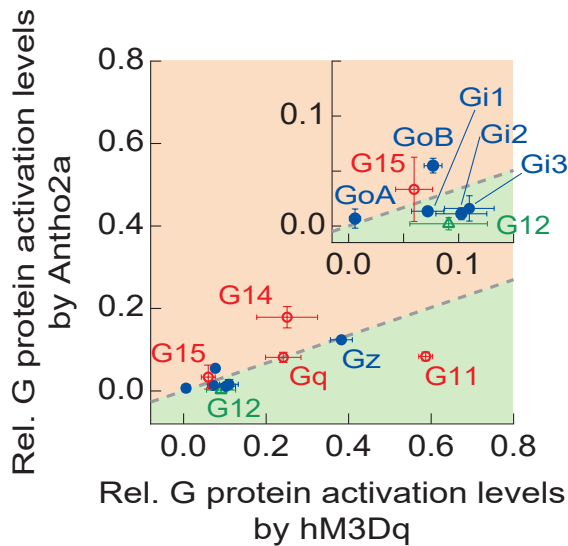
Fig. 6. Comparison of activation abilities between Antho2a with hM3Dq for various types of G proteins. Two-dimensional plots illustrate the activation levels of different types of G proteins by Antho2a compared to those by hM3Dq. G protein activation levels were measured using the NanoBiT-G-protein dissociation assay. The levels of G protein activation by Antho2a were plotted against those by hM3Dq. The activation levels for each G protein by Antho2a are represented by the maximum difference in the light-dependent decrease of relative luminescence (relative to baseline) between cells expressing both Antho2a and hM3Dq and those expressing only hM3Dq. Conversely, the activation levels for each G protein by hM3Dq are represented by the maximum difference in the agonist-dependent decrease between cells expressing both Antho2a and hM3Dq and those expressing only Antho2a. Measurements were performed for 11 different types of G proteins that were clearly activated by hM3Dq (see Supplementary Figure S5), including Gq group (red open circle), Gi group (blue solid circle), and G12 group (green open triangle) G proteins. Broken gray lines $y = f(x)$ represent straight lines passing through the origin and the point of Gq activation (green background: $y < f(x)$, orange background: $y > f(x)$). Circles or triangles with error bars indicate the mean $\pm$ SEM for $n = 3$ replicates. The inset shows an enlarged view of the figure.

indicating that their activation abilities relative to Gq are similar to or lower than those of hM3Dq (blue solid circles and green open triangles in Fig. 6).

The activation abilities of SpiRh1 and hM3Dq for each type of G protein were also comparatively investigated using the same methods as those applied for Antho2a and hM3Dq. We found that the activation abilities of SpiRh1 for three members of the Gq group (Gq, G11, G14) were roughly equivalent to those of hM3Dq (red open circles in Supplementary Figure S6). In contrast, the abilities of all members of the Gi group and G12 were plotted in the area of $y > f(x)$, indicating that SpiRh1 has higher activation abilities for these G proteins relative to Gq compared to hM3Dq, which is unlike Antho2a (blue solid circles and green open triangle in Supplementary Figure S6).

DISCUSSION

In this study, we found that two Antho2 opsins, Antho2a and Antho2d, from the ASO-II group in the reef-building coral *A. tenuis*, light-dependently activated Gq group G pro-

teins to increase Ca^{2+} in mammalian cultured cells. We previously reported that acropsin 4, an ASO-II group opsin from another coral species (*A. millepora*), also light-dependently elevates Ca^{2+} in mammalian cultured cells (Mason et al., 2023). Importantly, the *A. tenuis* genome (Shinzato et al., 2021) contains at least five different types of Gα proteins including Gαq, whose sequence of C-terminal five amino acids, known to be involved in selective interaction between Gα and a GPCR (Conklin et al., 1993; Blahos et al., 1998), is identical to that of mammalian Gq (see Supplementary Figure S7). Taken together, our findings suggest that members of the ASO-II group are generally Gq-coupled.

Accumulated experimental evidence has established that the protostome visual opsin/deuterostome melanopsin group is a large Gq-coupled opsin group (Koyanagi and Terakita, 2008). Human Opn5 was recently reported to couple with Gq (Wagdi et al., 2022), and more recently, the mammalian type Opn5 (Opn5m) has been shown to activate G14 from the Gq group (Sato et al., 2023). Based on our results, the ASO-II group can be regarded as a new Gq-coupled opsin group in addition to the known Gq-coupled opsin groups. Interestingly, regarding two well-studied opsins from the protostome visual opsin/deuterostome melanopsin group, jumping spider Rh1 (SpiRh1) activates members of Gi (Varma et al., 2019), while vertebrate melanopsins activate both Gi (Bailes and Lucas, 2013) and Gs (McDowell et al., 2022) members. Additionally, mouse and chicken Opn5s have been reported to activate Gi (Yamashita et al., 2010; Kojima et al., 2011) and we recently found that slug Opn5s activate Go (Matsuo et al., 2023). Interestingly, we found that Antho2d activates members of the Gi group in addition to those of Gq, similar to SpiRh1, while Antho2a activates members of the Gi group only slightly. As described above, the presence of Gs, Gi, Go, Gq, and G12/13 in the *A. tenuis* genome, each with C-terminal amino acid sequences identical or similar to their mammalian counterparts (see Supplementary Figure S7), suggests that the activation specificities of the Antho2 opsins toward these five types of G proteins, as observed in mammalian cultured cells, may generally reflect those in coral cells. However, further detailed discussions on the specific activation of G protein types and the physiological functions involving Antho2 opsins will require conducting NanoBiT-G-protein dissociation assays using coral G proteins and analyzing the co-localization of the Antho2 opsins and G proteins.

We observed the Gi/Go- and Gq-independent increase in cAMP levels in SpiRh1- and Antho2d-expressing cells, but not in Antho2a-expressing cells (Fig. 3). Previous studies revealed that Gs (Gilman, 1987) and G12/G13 (Jiang et al., 2008) serve as activators of cAMP synthesizing enzymes. However, neither SpiRh1 nor Antho2a activates Gs and G13, and both SpiRh1 and Antho2a activate G12 (see Supplementary Figure S2C, D). Therefore, activation of Gs and/or G12/G13 cannot account for the cAMP increase in the presence of Gi/Go as well as Gq inhibitors in SpiRh1-expressing cells but no cAMP increase in Antho2a-expressing cells. Further studies are necessary to investigate this unexplained increase in cAMP levels.

We found that Gi/Go activation contributes to the light-dependent Ca^{2+} elevation in Antho2d- and SpiRh1-expressing cells (Fig. 4). While Gi/Go activation is not essential for the light-dependent Ca^{2+} increase induced by

Antho2d or SpiRh1, it plays a significant additional role in enhancing the Ca^{2+} increase triggered by Gq activation. This is evidenced by the fact that the Gq inhibitor YM-254890 completely abolished the light-dependent Ca^{2+} increase in Antho2d- and SpiRh1-expressing cells (Fig. 2). Previous studies have shown that Gαq subunit from Gq (heterotrimeric G proteins including Gαq) and Gβγ subunit from Gi (heterotrimeric G proteins including Gαi) activated by Gq-coupled and Gi-coupled receptors, respectively, co-operatively increase the activity of PLCβ (possibly PLCβ3), leading to an enhanced increase in intracellular Ca^{2+} (Pfeil et al., 2020). In this study, we used PTX to clarify the contribution of Gi/Go to Ca^{2+} elevation in HEK293S cells expressing Antho2d or SpiRh1. It has been reported that HEK293S cells express a much larger amount of Gi compared to Go, whose mRNA expression levels are not clearly detected (Atwood et al., 2011). Therefore, it is reasonable to conclude that Antho2d and SpiRh1 activate Gi in cultured cells. We suggest that Antho2d and SpiRh1 function as both Gq- and Gi-coupled GPCRs, achieving Gi-dependent enhancement of the light-dependent Ca^{2+} increase caused by Gq activation. Thus, a possible explanation for the different PTX effect on Ca^{2+} response between Antho2d and SpiRh1 is that the relative activation efficiencies of Gq and Gi are different between Antho2d and SpiRh1. We should compare PTX effect and activation ratio of Gi and Gq to clarify the absolute effect of Gi for the enhancement of Gq cascade as our future study. However, while we have reported co-localization of SpiRh1 and Gq in the rhabdoms of visual cells in jumping spiders (Nagata et al., 2012), we have yet to clarify the co-localization of members of the Gi group with SpiRh1 or determine which subtype of PLCβ co-localizes with SpiRh1. Further studies are necessary to explore the co-operative activation of PLCβ by Gq and Gi.

In contrast to Antho2d and SpiRh1, Antho2a showed limited activation of members of the Gi group (Fig. 5B, and see Supplementary Figure S2B), while clearly activating members of the Gq group in cultured cells (Fig. 5A, and see Supplementary Figure S2A). Furthermore, we did not observe any enhancement of the Gq-mediated light-dependent increase in intracellular Ca^{2+} by Gi/Go activation (Fig. 4). The activation specificity of Antho2a for Gq is comparable to or even higher than that of hM3Dq, which is often used in chemogenetics due to its strong activation specificity for Gq. Therefore, we propose that Antho2a has potential as a Gq-manipulating GPCR optogenetic tool.

ACKNOWLEDGMENTS

COMPETING INTERESTS

The authors declare no competing interests.

AUTHOR CONTRIBUTIONS

MI, YS, MK, and AT conceived the study and designed research. MI, YS, and AT wrote the manuscript. MI, YS, T. Shirata, and T. Sugihara conducted experiments and analysis. All authors reviewed the manuscript.

SUPPLEMENTARY MATERIALS

Supplementary materials for this article are available online. (URL: https://doi.org/10.2108/zs240085)

Supplementary Figure S1. Wavelength-dependent increases in Ca^{2+} levels in Antho2d-expressing HEK293S cells.

Supplementary Figure S2. Time courses of G protein activation profiles measured by the NanoBiT-G-protein dissociation assay for Antho2a and SpiRh1.

Supplementary Figure S3. The effect of PTX on Gq activations by Antho2a and SpiRh1.

Supplementary Figure S4. The effects of YM-254890 and PTX on agonist-induced Ca^{2+} changes in hM3Dq-expressing HEK293S cells.

Supplementary Figure S5. Time courses of G protein activation by hM3Dq measured by the NanoBiT-G-protein dissociation assay.

Supplementary Figure S6. Comparison of activation abilities between SpiRh1 with hM3Dq for various types of G proteins.

Supplementary Figure S7. Comparison of C-terminal amino acid sequence between *A. tenuis* and human G protein alpha subunits.

REFERENCES

Armbruster BN, Li X, Pausch MH, Herlitze S, Roth BL (2007) Evolving the lock to fit the key to create a family of G protein-coupled receptors potently activated by an inert ligand. Proc Natl Acad Sci U S A 104: 5163–5168

Atwood BK, Lopez J, Wager-Miller J, Mackie K, Straiker A (2011) Expression of G protein-coupled receptors and related proteins in HEK293, AtT20, BV2, and N18 cell lines as revealed by microarray analysis. BMC Genomics 12: 14

Bailes HJ, Lucas RJ (2013) Human melanopsin forms a pigment maximally sensitive to blue light (λmax ≈ 479 nm) supporting activation of G(q/11) and G(i/o) signalling cascades. Proc R Soc B 280: 20122987

Blahos J, Mary S, Perroy J, De Colle C, Brabet I, Bockaert J, et al. (1998) Extreme C terminus of G protein α-subunits contains a site that discriminates between Gi-coupled metabotropic glutamate receptors. J Biol Chem 273: 25765–25769

Conklin BR, Farfel Z, Lustig KD, Julius D, Bourne HR (1993) Substitution of three amino acids switches receptor specificity of Gqα to that of Giα. Nature 363: 274–276

Dubinsky Z, Falkowski P (2011) Light as a source of information and energy in zooxanthellate corals. In "Coral Reefs: An Ecosystem in Transition" Ed by Z Dubinsky, Stambler, Springer Dordrecht, pp 107–118

Edgar RC (2004) MUSCLE: multiple sequence alignment with high accuracy and high throughput. Nucleic Acids Res 32: 1792–1797

Gilman AG (1987) G proteins: transducers of receptor-generated signals. Annu Rev Biochem 56: 615–649

Gohla A, Schultz G, Offermanns S (2000) Role for G(12)/G(13) in agonist-induced vascular smooth muscle cell contraction. Circ Res 87: 221–227

Gornik SG, Bergheim BG, Morel B, Stamatakis A, Foulkes NS, Guse A (2021) Photoreceptor diversification accompanies the evolution of Anthozoa. Mol Biol Evol 38: 1744–1760

Graham DM, Wong KY, Shapiro P, Frederick C, Pattabiraman K, Berson DM (2008) Melanopsin ganglion cells use a membrane-associated rhabdomeric phototransduction cascade. J Neurophysiol 99: 2522–2532

Hagio H, Koyama W, Hosaka S, Song AD, Narantsatsral J, Matsuda K, et al. (2023) Optogenetic manipulation of Gq- and Gi/o-coupled receptor signaling in neurons and heart muscle cells. eLife 12: e83974

Hering L, Mayer G (2014) Analysis of the opsin repertoire in the tardigrade *Hypsibius dujardini* provides insights into the evolution of opsin genes in panarthropoda. Genome Biol Evol 6: 2380–2391

Hubbard KB, Hepler JR (2006) Cell signalling diversity of the Gqα family of heterotrimeric G proteins. Cell Signal 18: 135–150

Inoue A, Raimondi F, Kadji FMN, Singh G, Kishi T, Uwamizu A, et al. (2019) Illuminating G-protein-coupling selectivity of GPCRs. Cell 177: 1933–1947.e25

Jiang LI, Collins J, Davis R, Fraser ID, Sternweis PC (2008) Regulation of cAMP responses by the G12/13 pathway converges on adenylyl cyclase VII. J Biol Chem 283: 23429–23439

Kayada S, Hisatomi O, Tokunaga F (1995) Cloning and expression of frog rhodopsin cDNA. Comp Biochem Phys B 110: 599–604

Kojima D, Mori S, Torii M, Wada A, Morishita R, Fukada Y (2011) UV-sensitive photoreceptor protein OPN5 in humans and mice. PLOS ONE 6: e26388

Koyanagi M, Terakita A (2008) Gq-coupled rhodopsin subfamily composed of invertebrate visual pigment and melanopsin. Photochem Photobiol 84: 1024–1030

Koyanagi M, Terakita A (2014) Diversity of animal opsin-based pigments and their optogenetic potential. Biochim Biophys Acta 1837: 710–716

Koyanagi M, Kubokawa K, Tsukamoto H, Shichida Y, Terakita A (2005) Cephalochordate melanopsin: evolutionary linkage between invertebrate visual cells and vertebrate photosensitive retinal ganglion cells. Curr Biol 15: 1065–1069

Koyanagi M, Nagata T, Katoh K, Yamashita S, Tokunaga F (2008) Molecular evolution of arthropod color vision deduced from multiple opsin genes of jumping spiders. J Mol Evol 66: 130–137

Koyanagi M, Takada E, Nagata T, Tsukamoto H, Terakita A (2013) Homologs of vertebrate Opn3 potentially serve as a light sensor in nonphotoreceptive tissue. Proc Natl Acad Sci U S A 110: 4998–5003

Koyanagi M, Shen B, Nagata T, Sun L, Wada S, Kamimura S, et al. (2022) High-performance optical control of GPCR signaling by bistable animal opsins MosOpn3 and LamPP in a molecular property-dependent manner. Proc Natl Acad Sci U S A 119: e2204341119

De La Fuente S, Fonteriz RI, De La Cruz PJ, Montero M, Alvarez J (2012) Mitochondrial free (Ca2^{+})dynamics measured with a novel low-Ca(2+) affinity aequorin probe. Biochem J 445: 371–376

Lee YJ, Shah S, Suzuki E, Zars T, O'Day PM, Hyde DR (1994) The Drosophila dgq gene encodes a G alpha protein that mediates phototransduction. Neuron 13: 1143–1157

Lilly E, Muscala M, Sharkey CR, McCulloch KJ (2024) Larval swimming in the sea anemone *Nematostella vectensis* is sensitive to a broad light spectrum and exhibits a wavelength-dependent behavioral switch. Ecol Evol 14: e11222

Mason BM, Koyanagi M, Sugihara T, Iwasaki M, Slepak V, Miller DJ, et al. (2023) Multiple opsins in a reef-building coral, *Acropora millepora*. Sci Rep 13: 1628

Matsuo R, Koyanagi M, Sugihara T, Shirata T, Nagata T, Inoue K, et al. (2023) Functional characterization of four opsins and two G alpha subtypes co-expressed in the molluscan rhabdomeric photoreceptor. BMC Biol 21: 291

McCoy KL, Traynelis SF, Hepler JR (2010) PAR1 and PAR2 couple to overlapping and distinct sets of G proteins and linked signaling pathways to differentially regulate cell physiology. Mol Pharmacol 77: 1005–1015

McCulloch KJ, Babonis LS, Liu A, Daly CM, Martindale MQ, Koenig KM (2023) *Nematostella vectensis* exemplifies the exceptional expansion and diversity of opsins in the eyeless Hexacorallia. Evodevo 14: 14

McDowell RJ, Rodgers J, Milosavljevic N, Lucas RJ (2022) Divergent G-protein selectivity across melanopsins from mice and humans. J Cell Sci 135: jcs258474

Molday RS, MacKenzie D (1983) Monoclonal antibodies to rhodopsin: characterization, cross-reactivity, and application as structural probes. Biochemistry 22: 653–660

Nagata T, Koyanagi M, Tsukamoto H, Saeki S, Isono K, Shichida Y, et al. (2012) Depth perception from image defocus in a jumping spider. Science 335: 469–471

Nagata T, Koyanagi M, Tsukamoto H, Mutt E, Schertler GFX, Deupi X, et al. (2019) The counterion-retinylidene Schiff base interaction of an invertebrate rhodopsin rearranges upon light activation. Commun Biol 2: 180

Oka Y, Saraiva LR, Kwan YY, Korsching SI (2009) The fifth class of Galpha proteins. Proc Natl Acad Sci U S A 106: 1484–1489

Pfeil EM, Brands J, Merten N, Vögtle T, Vescovo M, Rick U, et al. (2020) Heterotrimeric G protein subunit Gαq is a master switch for Gβγ-mediated calcium mobilization by Gi-coupled GPCRs. Mol Cell 80: 940–954.e6

Sakai Y, Kato K, Koyama H, Kuba A, Takahashi H, Fujimori T, et al. (2020) A step-down photophobic response in coral larvae: implications for the light-dependent distribution of the common reef coral, *Acropora tenuis*. Sci Rep 10: 17680

Sakai Y, Sen S, Sugihara T, Kakeyama Y, Iwasaki M, Schertler GFX, et al. (2025) Coral anthozoan-specific opsins employ a novel chloride counterion for spectral tuning. eLife (in press)

Sato K, Yamashita T, Ohuchi H (2023) Mammalian type opsin 5 preferentially activates G14 in Gq-type G proteins triggering intracellular calcium response. J Biol Chem 299: 105020

Shi Z, Tan ES, Takemura A (2024) Day-night expression patterns of opsin genes in the coral *Acropora digitifera* under natural and LED light conditions. In "Coral Reefs, Vol. 43", Ed by M Pratchett, Springer, pp 1535–1547

Shibahara S, Torruta Y, Sakakura T, Nager C, Chaudhuri B, Müller R (1986) Cloning and expression of cDNA encoding mouse tyrosinase. Nucleic Acids Res 14: 2413–2427

Shinzato C, Khalturin K, Inoue J, Zayasu Y, Kanda M, Kawamitsu M, et al. (2021) Eighteen coral genomes reveal the evolutionary origin of *Acropora* strategies to accommodate environmental changes. Mol Biol Evol 38: 16–30

Sugihara T, Nagata T, Mason B, Koyanagi M, Terakita A (2016) Absorption characteristics of vertebrate non-visual opsin, Opn3. PLOS ONE 11: e0161215

Sun L, Kawano-Yamashita E, Nagata T, Tsukamoto H, Furutani Y, Koyanagi M, et al. (2014) Distribution of mammalian-like melanopsin in cyclostome retinas exhibiting a different extent of visual functions. PLOS ONE 9: e108209

Taniguchi M, Nagai K, Arao N, Kawasaki T, Saito T, Moritani Y, et al. (2003) YM-254890, a novel platelet aggregation inhibitor produced by *Chromobacterium* sp. QS3666. J Antibiot (Tokyo) 56: 358–363

Terakita A (2005) The opsins. Genome Biol 6: 213

Terakita A, Nagata T (2014) Functional properties of opsins and their contribution to light-sensing physiology. Zool Sci 31: 653–659

Terakita A, Hariyama T, Tsukahara Y, Katsukura Y, Tashiro H (1993) Interaction of GTP-binding protein Gq with photoactivated rhodopsin in the photoreceptor membranes of crayfish. FEBS Lett 330: 197–200

Terakita A, Tsukamoto H, Koyanagi M, Sugahara M, Yamashita T, Shichida Y (2008) Expression and comparative characterization of Gq-coupled invertebrate visual pigments and melanop-

sin. J Neurochem 105: 883–890

Varma N, Mutt E, Mühle J, Panneels V, Terakita A, Deupi X, et al. (2019) Crystal structure of jumping spider rhodopsin-1 as a light sensitive GPCR. Proc Natl Acad Sci U S A 116: 14547–14556

Wagdi A, Malan D, Sathyanarayanan U, Beauchamp JS, Vogt M, Zipf D, et al. (2022) Selective optogenetic control of Gq signaling using human Neuropsin. Nat Commun 13: 1765

Yamashita T, Ohuchi H, Tomonari S, Ikeda K, Sakai K, Shichida Y (2010) Opn5 is a UV-sensitive bistable pigment that couples with Gi subtype of G protein. Proc Natl Acad Sci U S A 107: 22084–22089

Zhang H, Nielsen AL, Strømgaard K (2020) Recent achievements in developing selective Gq inhibitors. Med Res Rev 40: 135–157